Activated Carbon from Various Agricultural Wastes by Chemical Activation with KOH: Preparation and Characterization

Article *in* Journal of Biobased Materials and Bioenergy · June 2013

DOI: 10.1166/jbmb.2013.1379

CITATIONS
64

READS
6,833

6 authors, including:

Abdul Khalil H.P.S
Universiti Sains Malaysia
324 PUBLICATIONS **13,712** CITATIONS
SEE PROFILE

Mohammad Jawaid
Universiti Putra Malaysia
626 PUBLICATIONS **22,203** CITATIONS
SEE PROFILE

Ts. Dr. Umer Rashid
Universiti Putra Malaysia
330 PUBLICATIONS **9,133** CITATIONS
SEE PROFILE

Aminul Islam
Jessore University of Science and Technology
105 PUBLICATIONS **3,903** CITATIONS
SEE PROFILE

Journal of
Biobased Materials and Bioenergy
Vol. 7, 1–7, 2013

Activated Carbon from Various Agricultural Wastes by Chemical Activation with KOH: Preparation and Characterization

H. P. S. Abdul Khalil[1,*], M. Jawaid[2], P. Firoozian[1], Umer Rashid[3], Aminul Islam[4], and Hazizan Md. Akil[5]

[1] *School of Industrial Technology, Universiti Sains Malaysia, 11800 Penang, Malaysia*
[2] *Institute of Tropical Forestry and Forest Products (INTROP), Universiti Putra Malaysia, 43400 UPM Serdang, Selangor, Malaysia*
[3] *Institute of Advanced Technology, Universiti Putra Malaysia, 43400 UPM Serdang, Selangor, Malaysia*
[4] *Catalysis Science and Technology Research Centre, Faculty of Science, Universiti Putra Malaysia, 43400 UPM Serdang, Selangor, Malaysia*
[5] *School of Materials and Mineral Resources Engineering, Engineering Campus, Universiti Sains Malaysia, 14300 Nibong Tebal, Malaysia*

Activated carbons (AC) were prepared by pyrolysis from oil palm empty fruit bunch (EFB), bamboo stem (BS), and coconut shells (CNS) at 800 °C by using potassium hydroxide under nitrogen atmosphere. The influence of temperature and type of agricultural biomass on surface area and morphological properties investigated. Activated carbon produced from BS have a higher specific surface area (1212 m^2 g^{-1}) and microporosity percentage than those produced from oil palm EFB, and CNS lies in the range of commercial activated carbons. The morphological analysis of the samples was determined by scanning electron microscopy. The external surfaces are full of cavities and quite irregular as a result of activation. X-ray diffraction analysis showed degree of crystallinity 13.25% in case of AC-BS sample while AC-EFB and AC-CNS showed a crystallinity of 1.68% and 8.19%, respectively.

Keywords: Agricultural Biomass, Activated Carbon, Surface Area, Scanning Electron Microscopy, X-Ray Diffraction Analysis.

RESEARCH ARTICLE

1. INTRODUCTION

The gross supply of agricultural biomass arises from different sources during production of food and feed are increasing around the world. Lignocellulosic biomass is one of the potential sustainable materials for producing energy and chemical feedstocks.[1] Carbon may be obtained from various sources and may have varied surface area, porosity, and other properties. The physical properties depend on (1) Type of starting material, (2) Procedure chosen for preparation of the product, and (3) Conditions under which it used. Agricultural waste biomass such as oil palm EFB, coconut shells, rice husk, bamboo stem, etc. has gained much attention over the last decade for the production of activated carbons (AC) by thermo-chemical conversion.[2] The economical and technical advantages transformation utilization of biomass which affect the storage, transportation, processing and utilization of this energy source.[3] These criteria can help to produce activated carbon with different properties.[4] Three type of activated carbon prepared by chemical activation of cork powder waste using KOH as activating agent.[5] Activated carbon process by various methods such as without any activation procedure, template methods to obtain microporous or mesoporous carbons,[6,7] and defluorination of polytetrafluoroethylene[8] to give mesoporous carbons, etc. KOH activated lignocellulosic materials such as coconut shells and palm stones were used for increasing the mesoporosity.[9] The most common raw materials used for the production of activated carbons such as rice husk,[10] grape seed,[11] waste tyres,[12] hazelnut shell[13] etc.

Researchers use the three parts of Manihot stems residues to obtain different materials and characterize and

*Author to whom correspondence should be addressed.
Email: akhalilhps@gmail.com

employ them as precursors of carbon.[14] Activated carbon used since prehistoric age and played a pivotal role in many fields. Since, the discovery of activated carbon (AC), there has been remarkable interest in its synthesis due to its remarkable adsorptive, environmental, thermal, electrical and mechanical characteristics. It's proof from previous study that activated carbon is one of the leading industrial materials due to its well developed pore structure and adsorption properties.[15] Recent developments in modern technologies have resulted in various novel applications of activated carbons. Researchers reported the influence of interfacial structure on interfacial properties between activated carbon filler and organic matrix of composites.[16] However, the high surface area and porosity are the prerequisite for the activate carbon. It was reported that the carbon activated with potassium hydroxide (KOH) provided surface area as high as 3000 m^2/g.[17]

The main objective of the present study is to do preparation and characterization of elemental analysis, surface area, and morphological properties of ACs from oil palm EFB, bamboo stem, and coconut shells by using KOH as activating agent. In view of the aforementioned, further objective of this study was to investigate the potential of activated carbon-bamboo stem (AC-BS), activated carbon-oil palm EFB (AC-EFB), and activated carbon-coconut shells (AC-CNS) by using KOH as the nanofiller for epoxy composites.

2. MATERIALS AND METHODOLOGY

2.1. Materials

Waste biomass EFB sample obtained from Ecofuture Berhad, Malaysia, Bamboo stem supplied by Forest Research Institute Malaysia (FRIM), and coconut shell procured from Anjung Juara Sdn, Bhd, used without further treatments. Potassium hydroxides (KOH) (~85% alkali) obtained from R&M Chemical Essex, UK. All chemicals used in the investigation were of analytical grade. Morphological, chemical, and thermal properties of raw materials (oil palm EFB, bamboo stem, and coconut shells) reported in our previous work.[18]

2.2. Preparation of Activated Carbon Under Alkali Reagent

The raw materials (EFB, BS, and CNS) preparation was similar to as mentioned in our previous research.[18] About 200g each of dried raw materials were impregnated in potassium hydroxide in 1:3 ratio, and heated in a water bath at 85–90 °C for 24 h. The sample was then placed in a stainless steel vertical tubular reactor and put in the furnace. The pyrolysis process was similar to as mentioned in our previous research[19] at 800 °C under the pressure of 1 atmosphere, for 2 h. The obtained product was cooled to room temperature (30 °C), washed with distilled water, and then dried in an oven at 100 °C for 2–4 h.[20]

2.3. Characterization of Activated Carbon

2.3.1. Carbon Hydrogen Nitrogen (CHN)

The elemental compositions carbon (C), hydrogen (H), and nitrogen (N) contents of materials were analyzed using a CHN analyzer (Perkin Elmer Series II 2400).

2.3.2. Surface Area Analysis

The specific surface area, pore volume, and pore size distribution of the activated carbon were determined from the adsorption isotherms using Brunauer–Emmett–Teller (BHT)[21] equation and Quantachrome Nova Win2© 1994–2002 instrument. The cross-sectional area of a nitrogen molecule is assumed to be 0.162 nm. The Dubinin–Radushkevich (DR) equation was used to calculate the micropore volume. The total pore volume was estimated to be the liquid volume of the adsorbate (N_2) at a relative pressure of 0.985. The pore size distribution was determined using the BJH model. The average pore diameter was calculated as 4 times the total pore volume over the BET surface area.

2.3.3. Scanning Electron Microscopy (SEM)

Morphological studies of the samples were carried out using a Leica Cambridge S-360 scanning electron microscopy (SEM). The samples were mounted onto a SEM holder with double-sided electrically-conducting carbon-adhesive tabs to prevent the surface of the specimens when exposed to the electron beam. The samples were then coated with a 20 nm thick layer of gold using a Polaron Equipment Limited model E500, set at a voltage of 1.2 kV (10 mA) and a vacuum 20 Pa for 10 min.

2.3.4. Fourier Transform Infra-Red (FT-IR) Analysis

A FT-IR spectrophotometer measured in a Nicolet Avatar Model 360 instrument using potassium bromide (KBr) pellet for wavelength ranged from 4000 to 400 cm^{-1}. FT-IR spectra were obtained with dried powdered samples recorded as KBr disks on a Nicolet AVATAR 360 Fourier Transform Infrared Spectrophotometer. Approximately 1 mg samples were mixed in a matrix of KBr (100 mg) and pressed to form pellets.

2.3.5. X-Ray Diffraction Analysis (XRD)

X-ray diffraction analysis was performed on activated carbon in order to determine the degree of crystalline or amorphous nature of the AC. Analyses were performed by Philips PW1050 X-pert diffractometer using Cu-Kα (= 0.15406 Å) radiation source operating under a voltage of 40 kV and a current of 25 mA. The diffraction angle (2θ) was varied from 2.5° to 10°. Activated carbons were analyzed for their orientation within the matrix material.

The diffractograms were analyzed by X-pert High Score Plus Software. The X-ray diffraction patterns were collected with a scan rate of 4.2 °C/min.

Degree of crystallinity of samples was quantitatively estimated following the method of Wang.[35] The equation of the degree of crystallinity is as follows:

$$\chi_c = \frac{A_c}{(A_c + A_a)} \quad (1)$$

Where: X_c refers to the degree of crystallinity;

A_c refers to the crystallized area on the X-ray diffractogram;

A_a refers to the amorphous area on the X-ray diffractogram.

3. RESULTS AND DISCUSSION

3.1. Abbreviations of Activated Carbons

The chemically activated carbon samples obtained from oil palm empty fruit bunch (EFB), bamboo stem (BS) and coconut shell (CNS) were named as AC-EFB, AC-BS, and AC-CNS, respectively. In this study potassium hydroxides used as activating agent for preparation of AC. So, we abbreviated activated carbon samples of oil palm EFB, bamboo stem, and coconut shells as AC-EFB K, AC-BS K, and AC-CNS K, respectively.

3.2. Elemental Analysis (CHN)

CHN values of activated carbon prepared by using chemical reagent (KOH) shown in Table I. The carbon content of AC-CNS was the highest in all the three samples by KOH chemical reagents while percentage of carbon content in AC-BS is the lowest. Activated carbon obtained from CNS shows higher percentage of carbon (83.9%), while AC-EFB appraises lower percentage of hydrogen (1.09%) and AC-BS lowest percentage of nitrogen content (0.10%). Carbon content of raw materials in the range of 44.2–49.2% which is lower than carbon content of char produced from EFB, BS, and CNS (Table I). These results are comparable to Seredych's[22] work on commercial activated carbon from coconut shell wherein similar carbon content higher than 79% is reported.

3.3. Surface Area Analysis (S_{BET})

In the present study by using KOH, most surface areas were greater than 600 m^2/g, which is comparable to commercial activated carbon and mass recovery yields of 20.7% (Table II). The yield of black walnut shells, 24% and macadamia nutshells and hazelnut shells 21%, reported[2] which were in agreement with Table II. Pore size distribution (Fig. 2) calculated based on their N_2 adsorption isotherm (Fig. 1). The comparison of apparent specific surface area for samples- AC-EFB K, AC-BS K and AC-CNS K, showed that chemical activation seems to improve the development of porosity.[23]

Table II. Surface area and Yield of the AC-K.

	S_{BET} (m^2/g)	S_{Lang} (m^2/g)	Yield
AC-EFB K	663	1122	17.8%
AC-BS K	726	1222	19.6%
AC-CNS K	636	987	20.7%
Cherry Stones[42]	1167	–	–
Wood-based AC[43]	2300	–	–
Cotton stalk[44]	997	1311	–

Figure 1 shows the adsorption/desorption isotherm data of nitrogen on three different activated carbons by using KOH. An attempt has also been made to understand the mechanism of adsorption of activated carbon. In Figure 3, the adsorption isotherms of AC-BS K, AC-EFB K, and AC-CNS K presented for comparison purposes. It is clear that nitrogen isotherms of KOH activated carbon show significant increment in nitrogen adsorption at low, middle, and high relative pressures. Therefore, isotherms of three activated carbons shaped as a combination of Type I. The three main parameters of an adsorbent that influence its adsorptive behaviour are its porosity, surface area, and surface groups.[24] AC-BS K exhibit a steep Type I isotherm at low pressure and less steep, Type I isotherm with slightly sloped up plateau at higher relative pressures. The KOH activation of bamboo based char at the char/KOH ratio of 1:3 induces a relatively high mesopore fraction.[25] AC-CNS K exhibit a steep Type I isotherm with an almost horizontal plateau. AC-EFB K has a large amount of nitrogen that adsorbed at high relative pressures. The plateau of this isotherm commences at high relative pressures (p/p_o), and towards the end of isotherm, steep gradient seen as a result of limited nitrogen uptake which indicate capillary condensation in the mesopores.[22] Hamad et al.[20] reported that above 750 °C the mesopores are more pronounced, and thermal degradation of pore wall occurs causing the widening of micropores. According to the results of the S_{BET} the external surface area reported 199.16, 140.99 and 71.49 (m^2/g) for AC-BS K, AC-EFB K and AC-CNS K, respectively.[20]

Table I. Comparison of CHN values of activated carbon using KOH.

	AC-EFB K	AC-BS K	AC-CNS K	EFB[18]	BS[18]	CNS[18]
Carbon (%)	80.47	79.11	83.91	44.2	45.9	49.2
Hydrogen (%)	1.09	1.60	1.28	5.8	5.9	6.2
Nitrogen (%)	0.14	0.10	0.12	0.2	0.2	0.3

RESEARCH ARTICLE

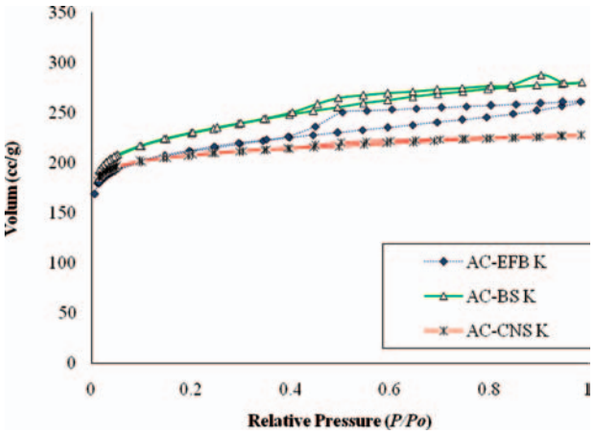

Fig. 1. Adsorption isotherm of nitrogen on activated carbons, Upper lines are desorption of each component (by using KOH) Pore diameter.

Figure 2 shows pore size distributions of activated carbons samples extracted by using KOH activating agent. From Figure 4, it is obvious that mesoporosity in AC-EFB K developed nicely, but AC-BS K show moderate development as compared to the AC-CNS K with decidedly less mesoporosity. It may be noted that activated carbon produced from BS has higher specific surface area and microporosity percentage than those produced from EFB and CNS. This may be due to the difference in chemical composition of raw materials.[18] Hu et al.[26] reported that the pore size distribution is dependent largely on the degree of chemical impregnation.

The yield of the activated carbon at carbonization temperatures of more than 700 °C are less than fixed carbon in initial precursor[18] because KOH is the strong base it catalyses the oxidation reactions therefore more carbon atom in the surface oxidized leading to widening of the pore structures. When the same pyrolysis and activation conditions applied to two different samples of the same nutshell, the mass yields, surface areas, micropore, and mesopore volumes were within 5% of each other, therefore satisfactory reproducibility achieved.[2] Normally, carbon with high-porosity can be obtained at high extent of char burn-off leading to a low production yield. The pyrolysis process caused a decrease in the percentage yield while the S_{BET} surface area increased progressively.[27]

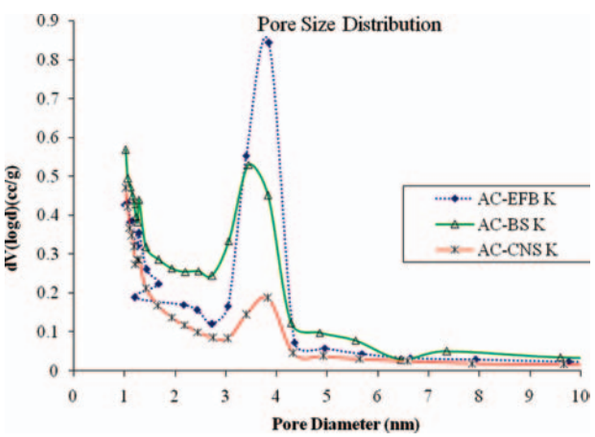

Fig. 2. Pore size distribution of activated carbon AC-BS K, AC-EFB K, and AC-CNS K.

3.4. Scanning Electron Microscopy (SEM)

SEM macrographs (Figs. 3(a)–(c)) show that the external morphology of the activated carbon at the pyrolysis

(a) SEM at a magnification (1 × 5000) of AC-BS K

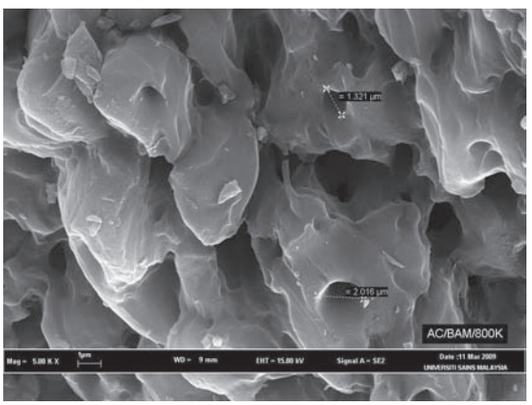

(b) SEM at a magnification (1 × 5000) of AC-EFB K

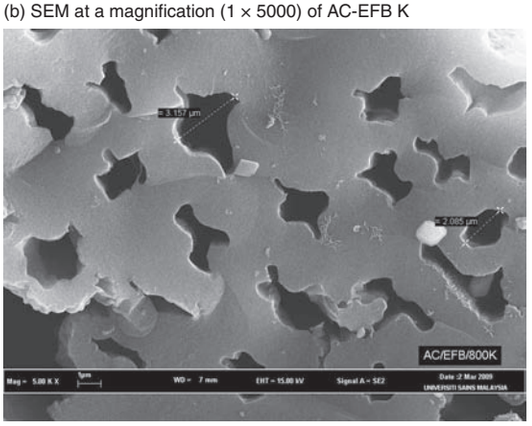

(c) SEM at a magnification (1 × 5000) of AC-CNS K

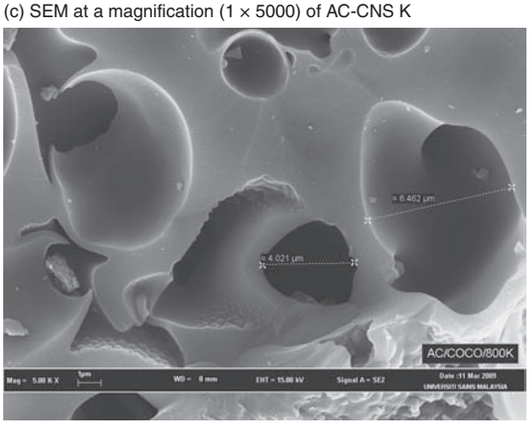

Fig. 3. SEM at a magnification (1 × 5000) of (a) AC-BS K, (b) AC-EFB K, and (c) AC-CNS K.

RESEARCH ARTICLE

(a) SEM at a magnification 1 × 1000 of AC-BS K after ball milling

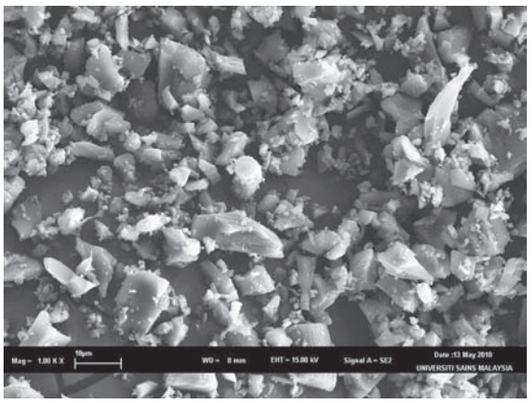

(b) SEM at a magnification 1 × 1000 of AC-EFB K after ball milling

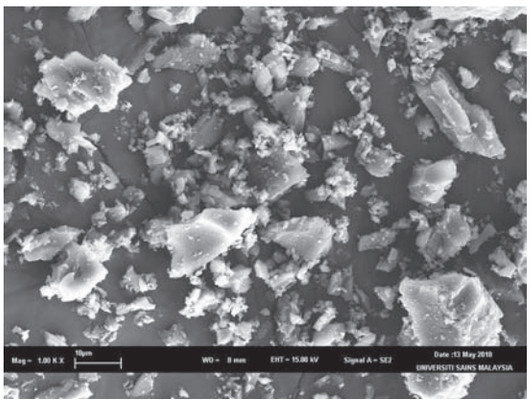

(c) SEM at a magnification 1 × 1000 of AC-CNS K after ball milling

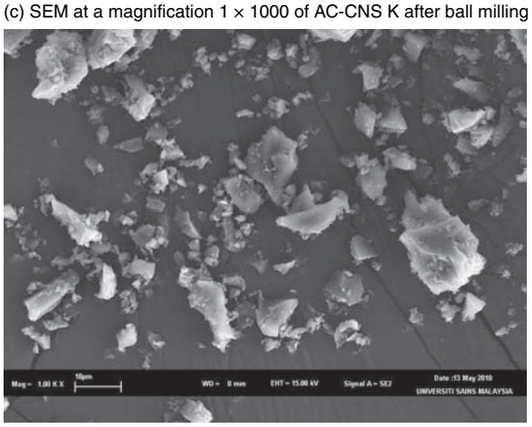

Fig. 4. SEM at a magnification 1 × 1000 of (a) AC-BS K (b) AC-EFB K (c) AC-CNS K after ball milling.

temperature of 800 °C more intact as compared with other activated carbons. The surface of the samples found to be relatively organized without any pores except for some occasional cracks as compared to raw materials. Pyrolysis at 800 °C under the pressure of 1 atm, for 2 h produced activated carbon with undulating surface (Figs. 3(a)–(c)). There are many clear fine pores visible within the microstructure of activated carbons. The SEM images of the three-activated carbons; AC-BS K, AC-EFB K and AC-CNS K showed that the external surfaces for these carbons are full of cavities and quite irregular as a result of activation. There are numerous cracks and small pits distributed over the surface, indicating the severe interaction of the KOH with agricultural wastes during carbonization.[28] The presence of micropore and mesopore in the three-activated carbons; AC-BS K, AC-EFB K and AC-CNS K illustrate the difference from raw materials from agricultural wastes in our previous study.[18]

There are many thin sheets or layers within the structure, between which are some rudimentary pores due to the release of volatiles. Activation at 800 °C with KOH resulted in the creation of more pores and a substantial removal of volatiles.[29] The white spheres and some fluffy materials may be due to the presence of KOH residues and some other impurities. A system of advanced pore network formed in case of AC-CNS K as compared to the other two AC-BS K and AC-EFB K, since there were no more lignocellulosic structures on the surface of AC-CNS K. Due to these well developed pores in activated carbon possessed high surface area. Because the KOH reagent is a strong base due to that it able to interact with carbon atoms and thus, catalyse the dehydrogenation and oxidation reaction, leading to the increment of tar evolution and development of porosity.[30] In the present study, raw materials/KOH in the ratio of 1:3 used. It is reported in literature finding that larger ratio of KOH probably forms an insulating layer, covering the particles, thus reducing the activation process and contact with the surrounding environment.[31]

S_{BET} results after ball-milling show no significant enhancement in surface area.[18] The result of the scanning electron microscopy (Fig. 4) shows that there are a few particles higher than 1 mm. It appears that ball milling did not change the surface area of the powder but simply changed the ratio of physisorbed gas to chemisorbed gas which is in accordance with previous result.[32] It also clear that longest milling time leads to agglomeration of the smaller particles into these large particles. It evident that the formation of the smallest particles (<100 nm) greatly enhanced during this period of ball-milling.

3.5. FT–IR Spectra of Activated Carbon

The adsorption capacity of activated carbon depends upon porosity as well as the chemical reactivity of functional groups at the surface. The knowledge on surface functional groups would give insight to the adsorption capability of the activated chars produced.[33] FT–IR spectra collected for qualitative characterization of surface functional groups of activated carbons. IR spectroscopy is another method that has been employed to identify the functional groups present on activated carbon surfaces.[34]

The FT–IR spectra of the activated carbon prepared by using KOH activating agent shown in Figure 5. The band around 3430 cm^{-1} assigned to the O—H stretching

RESEARCH ARTICLE

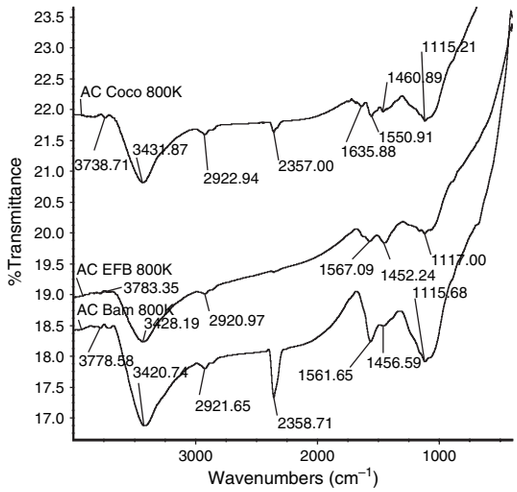

Fig. 5. FT-IR spectra of AC-EFB K, AC-BS K, and AC-CNS K.

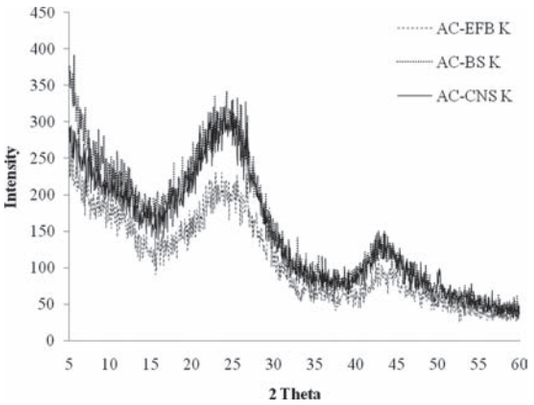

Fig. 6. X-ray diffraction of the activated carbon with KOH.

vibration mode of hydroxyl functional groups in AC-BS K, AC-EFB K, and AC-CNS K. The methylene group detected by C—H stretching at a wave number of 2922 cm^{-1} in AC-CNS K while it observed at 2920 cm^{-1}, 2921 cm^{-1} in AC-EFB K, and AC-BS K, respectively. The band visible at 2360–2361 cm^{-1} corresponds to the stretching vibration of the C–O for carbon monoxide or carbon dioxide derivatives in AC-BS K, and AC-CNS K.

3.6. X-Ray Diffraction Analysis (XRD)

XRD is the most useful method to see the nano-particle size and crystalline and amorphous materials. Researchers worked on X-Ray Diffraction analysis of activated carbons, concluded that predominantly amorphous solid having large internal surface area and pore volume.[27] It found that activated carbon showed very disordered microcrystalline structure in which graphitic microcrystals are randomly oriented.[37]

Table III showed the degree of crystallinity in the activated carbon powder. Figure 6 showed that the AC-K in case of BS is high where as the crystallinity of AC-BS is 13.25%. AC-CNS K and AC-EFB K showed a crystallinity of 8.19% and 1.68%, respectively. In all these cases AC treated with KOH showed less crystallinity, it means that samples are semi crystalline or amorphous. In case of activated carbon, several researchers reported that activated carbon to be amorphous materials.[37–39] Activated carbon, generally regarded as an amorphous carbon, has a large surface area and porosity.[40] Two weak diffraction maxima indicated that the content of ordered crystalline phase is negligible. It was reported that XRD patterns for each of the activated carbon indicated a shape of typical amorphous carbon and showed broad asymmetric peaks corresponding to $2\theta \sim 25°$ and $2\theta \sim 50°$. This assumption is consistent with the images of scanning electron micrograph of activated carbons shown in Figures 3(a)–(c). These SEM images revealed that the origin of three activated carbons is from carboniferous material and represented amorphous carbon having many pores in common, but only AC-CNS showed quite different shape.[41]

Table III. Variation of percentage crystallinity of the nano AC.

Sample	AC by KOH
AC-BS	13.25
AC-EFB	1.68
AC-CNS	8.19

4. CONCLUSIONS

The carbon content of coconut shell was the highest in all the three samples while carbon content (%) of AC-BS is the lowest. Activated carbons produced from bamboo stem have a higher specific surface area (726 m^2/g) and microporosity percentage than those produced from EFB and coconut shells. The SEM images of the three-activated carbons; AC-BS K, AC-EFB K, and AC-CNS K showed that the external surfaces for these carbons are full of cavities and quite irregular as a result of activation. AC obtained by using KOH show higher mesopore, and contains relative high percentage of carbon. The FT–IR spectroscopy showed presence of significantly different peak frequencies in all the three activated carbons by different functional groups. The XRD results confirmed that AC treated with KOH showed less crystallinity.

Acknowledgment: Authors would like to thanks the Universiti Sains Malaysia, Penang for providing the research facilities that has made this work possible.

References

1. F. Lu and J. Ralph, *J. Biobased Mater. Bio.* 5, 169 (**2011**).
2. D. An, Y. Guo, B. Zou, Y. Zhu, and Z. Wang, *Biomass Bioenerg.* 35, 1227 (**2011**).

3. G. San Miguel, J. Makibar, and A. R. Fernandez-Akarregi, *J. Biobased Mater. Bio.* 6, 193 **(2012)**.
4. L. H. Wartelle, W. E. Marshall, C. A. Toles, and M. M. Johns, *J. Chromatogr. A* 879, 169 **(2000)**.
5. B. Cardoso, A. S. Mestre, A. P. Carvalho, and Joaõ Pires, *Ind. Eng. Chem. Res.* 47, 5841 **(2008)**.
6. Z.-G. Shi, Y.-Q. Feng, L. Xu, and S.-L. Da, *Carbon* 41, 2668 **(2003)**.
7. T. Morishita, Y Soneda, T. Tsumura, and M. Inagaki, *Carbon* 44, 2360 **(2006)**.
8. T. Yamamoto, T. Nishimura, T. Suzuki, and H. Tamon, *Carbon* 39, 2374 **(2001)**.
9. Z. Hu, H. Guo, M. P. Srinivasan, and N. Yaming, *Sep. Purif. Technol.* 31, 47 **(2003)**.
10. Y. P. Guo, J. Z. Zhao, H. Zhang, and S. F. Yang, *Dyes Pigment* 66, 123 **(2005)**.
11. D. Ozcimen and A. Ersoy-Mericboyu, *J. Hazard. Mater.* 168, 1118 **(2009)**.
12. G. Lopez, M. Olazar, M. Artetxe, M. Amutio, G. Elordi, and J. Bilbao, *J. Anal. Appl. Pyrol.* 85, 539 **(2009)**.
13. E. Demirbas, M. Kobya, and S. Oncel, *Bioresour. Technol.* 84, 291 **(2002)**.
14. C. M. Antonio-Cisneros and M. P. Elizalde-Gonza' lez, *Biomass Bioenerg.* 34, 389 **(2010)**.
15. A. H. Basta, V. Fierro, H. El-Saied, and A. Celzard, *Bioresource Technol.* 100, 3941 **(2009)**.
16. T. Travinskaya, A. Perekhrest, Y. Savelyev, N. Kanellopoulos, K. Papadopoulos, and K. Agiamarnioti, *Appl. Surf. Sci.* 256, 4391 **(2010)**.
17. N. Rie, N. Yoko, O. Naoto, and I. Michio, *New Carbon Mater.* 21, 289 **(2006)**.
18. H. P. S. Abdul Khalil, P. Firoozian, I. O. Bakare, H. M. Akil, and A. M. Noor, *Mater. Design* 31, 3419 **(2010)**.
19. P. Firoozian, I. U. H. Bhat, H. P. S. A. Khalil, A. M. Noor, H. M. Akil, and A. H. Bhat, *Mater Technol.* 26, 222 **(2011)**.
20. B. K. Hamad, A. M. Noor, A. R. Afida, and M. N. Mohd Asri, *Desalination* 257, 1 **(2010)**.
21. E. Gomibuchi, T. Ichikawa, K. Kimura, S. Isobe, K. Nabeta, and H. Fujii, *Carbon.* 44 983 **(2006)**.
22. M. Seredych and T. J. Bandosz, *J. Phys. Chem. C* 112, 4704 **(2008)**.
23. M. Ahmedna, W. E. Marshall, and R. M. Rao, *Bioresource Technol.* 71, 103 **(2000)**.
24. C. Michailof, G. G. Stavropoulos, and C. Panayiotou, *Bioresource Technol.* 99, 6400 **(2008)**.
25. S. B. Kim, T. Inoue, A. Shimizu, and S. Murase, *Physica C* 445, 1119 **(2006)**.
26. Z. Hu, M. P. Srinivasan, and Y. Ni, *Carbon.* 39, 877 **(2001)**.
27. A. B. J. Nurul, The Production and Characterization of Activated Carbon Using Local Agricultural Waste through Chemical Activation Process: Ph.D. Thesis, Universiti Sains Malaysia, Penang **(2007)**.
28. A.-N. A. El-Hendawy, A. J. Alexander, R. J. Andrews, and G. Forrest, *J. Anal. Appl. Pyro.* 82, 272 **(2008)**.
29. A. C. Lua and T. Yang, *Carbon* 42, 219 **(2004)**.
30. L. Hsu and H. Teng, *Fuel Process. Technol.* 64, 155 **(2000)**.
31. B. S. Girgis and A. N. A. El-Hendawy, *Micropor. Mesopor. Mat.* 52, 105 **(2002)**.
32. N. J. Welham, V. Berbenni, and P. G. Chapman, *Carbon* 40, 2307 **(2002)**.
33. V. Sricharoenchaikul, C. Pechyen, D. Aht-Ong, and D. Atong, *Energ. Fuel.* 22, 31 **(2008)**.
34. M. Olivares-Marín, C. Fernández-González, A. Macías-García, and V. Gómez-Serrano, *Energ Fuel.* 21, 2942 **(2007)**.
35. J. Sánchez-González, A. Macías-García, M. F. Alexandre-Franco, and V. Gómez-Serrano, *Carbon.* 43, 741 **(2005)**.
36. K. Babel and K. Jurewicz, *Carbon.* 46, 1948 **(2008)**.
37. A. R. Mohamed, M. Mohammadi, and G. N. Darzi, *Renew Sust. Energ. Rev.* 14, 1591 **(2010)**.
38. A. W. M. Ip, J. P. Barford, and G. McKay, *Bioresource Technol.* 99, 8909 **(2008)**.
39. M.-W. Jung, K.-H. Ahn, Y. Lee, K.-P. Kim, J.-S. Rhee, J. Tae Park, and K.-J. Paeng, *Microchem. J.* 70, 123 **(2001)**.
40. M. Olivares-MarÃn, C. FernÃ!ndez-GonzÃlez, A. MacÃas-GarcÃa, and V. GÃ³mez-Serrano, *Appl. Surf. Sci.* 252, 5980 **(2006)**.
41. I. I. Salame and T. J. Bandosz, *Ind. Eng. Chem. Res.* 39, 301 **(2000)**.
42. A.-N. A. El-Hendawy, A. J. Alexander, R. J. Andrews, and G. Forrest, *J. Anal. Appl. Pyrol.* 82, 272 **(2008)**.

Received: 5 September 2012. Accepted: 21 April 2013.

RESEARCH ARTICLE